

See discussions, stats, and author profiles for this publication at: <https://www.researchgate.net/publication/23233383>

TiO₂ Photocatalysis of Natural Organic Matter in Surface Water: Impact on Trihalomethane and Haloacetic Acid Formation Potential

ARTICLE *in* ENVIRONMENTAL SCIENCE AND TECHNOLOGY · SEPTEMBER 2008

Impact Factor: 5.33 · DOI: 10.1021/es800887s · Source: PubMed

CITATIONS

71

READS

30

6 AUTHORS, INCLUDING:



Sanly Liu

University of New South Wales

20 PUBLICATIONS 317 CITATIONS

SEE PROFILE



Mary Drikas

SA Water

114 PUBLICATIONS 2,297 CITATIONS

SEE PROFILE



Rose Amal

University of New South Wales

333 PUBLICATIONS 9,691 CITATIONS

SEE PROFILE

TiO₂ Photocatalysis of Natural Organic Matter in Surface Water: Impact on Trihalomethane and Haloacetic Acid Formation Potential

SANLY LIU,[†] MAY LIM,[†]
ROLANDO FABRIS,[‡]
CHRISTOPHER CHOW,[‡] MARY DRIKAS,[‡]
AND ROSE AMAL^{*,†}

ARC Centre of Excellence for Functional Nanomaterials,
School of Chemical Sciences and Engineering, The University
of New South Wales, Sydney NSW 2052, Australia, and CRC
for Water Quality and Treatment, Australian Water Quality
Centre, South Australian Water Corporation,
Bolivar SA 5110, Australia

Received March 30, 2008. Revised manuscript received
May 24, 2008. Accepted June 10, 2008.

In this study, changes in the physical and structural properties of natural organic matter (NOM) during titanium dioxide photocatalytic oxidation process were investigated using several complementary analytical techniques. Potential of the treated water to form trihalomethanes (THMs) and haloacetic acids (HAAs) was also studied. High-performance size exclusion chromatography analysis showed that NOM with apparent molecular weights of 1–4 kDa were preferentially degraded, leading to the formation of lower molecular weight organic compounds. Resin fractionation of the treated water demonstrated that the photocatalytic oxidation changed the affinity of the bulk organic character from predominantly hydrophobic to more hydrophilic. Short chain aldehydes and ketones were identified by mass spectroscopy as one of the key degradation products. The addition of hydrogen peroxide to photocatalysis was found to increase the degradation kinetics but did not affect the reaction pathway, thus producing similar degradation end products. The amount of THMs normalized per dissolved organic carbon (specific THM) formed upon chlorination of NOM treated with photocatalytic oxidation was reduced from 56 to 10 $\mu\text{g}/\text{mg}$. In contrast, the specific HAAs formation potential of the treated water remained relatively unchanged from the initial value of 38 $\mu\text{g}/\text{mg}$, which could be due to the presence of hydrophilic precursor compounds that were formed as a result of the photocatalytic oxidation process.

Introduction

Natural organic matter (NOM) is ubiquitous in surface water and groundwaters. It is formed from the decomposition of plant and animal residues and from microbial activity (1). NOM in drinking water supplies poses significant concerns to the water utility since it can cause color, taste, and odor problems in the finished water. NOM can also interfere with several water treatment processes, such as activated carbon

adsorption (2), membrane filtration (3), or ion exchange. In addition, NOM is known to react with chlorine during the water disinfection process to form disinfection byproducts (DBPs), such as trihalomethanes (THMs) and haloacetic acids (HAAs), which are potentially carcinogenic (4).

An effective and commonly applied method to decrease the concentration of DBPs is to eliminate the reaction between organic molecules and chlorine by removing NOM prior to disinfection. NOM is composed of a heterogeneous mixture of humic substances, carboxylic acids, proteins, amino acids, hydrocarbons, and polysaccharides (5). The physical and chemical nature of NOM varies according to the water source, age, and season (6). Therefore, aquatic NOM is a challenging contaminant to remove.

At present, methods to remove NOM in drinking water treatment include coagulation (7), ion exchange (8), membrane filtration (9), and activated carbon adsorption (10). The current need to further improve water quality has driven research on advanced oxidation processes (AOPs) such as ozone (11) and/or hydrogen peroxide (12), with or without being photoassisted with UV light. It has also been reported that the combination of treatment processes has resulted in an improved removal efficiency of NOM compared to that of processes in isolation (13, 14).

An additional option in AOPs is the application of titanium dioxide (TiO₂) photocatalytic treatment. TiO₂ oxidation has been shown to be effective in the destruction of NOM (15, 16). The use of titanium dioxide-based photocatalytic treatment is particularly attractive due to the potential to degrade the organic macromolecules, instead of merely capturing and transferring them to another phase, as in the case of more conventional removal processes.

While parameters affecting the TiO₂ photocatalytic oxidation of NOM have been studied extensively (16–19), relatively little information is available on how the process changes the nature and composition of the organic matter. These are important considerations in the practical design and development of photocatalytic treatment processes for NOM removal. A variety of byproducts are also produced during the course of the treatment process, some of which can be more recalcitrant or toxic than the parent compound.

The isolation and chemical analysis of aquatic NOM itself is a challenging task due to the complexity and heterogeneous nature of NOM. The identity of the constituent compounds often remains unknown and several techniques in tandem are often required to generate a comprehensive understanding of the composition and physical properties of NOM (20). Most photocatalytic studies of NOM attempted to monitor the changes in dissolved organic carbon (DOC) concentration and UV absorbance at 254 nm (UV₂₅₄) in the water. However, these analytical techniques may not be adequate to fully understand the effect of photocatalytic treatment on NOM since they are generalized parameters for determining the overall quality of drinking water.

We have previously reported the use of several complementary analytical techniques to study the effect of TiO₂ photocatalysis on the transformation and removal efficiency of humic acid (21). As an extension to the previous work, this paper presents a detailed examination on the evolution of NOM in a surface water sample during photocatalytic treatment. High-performance size exclusion chromatography (HPSEC) and resin fractionations are used to classify the NOM components into more specific subgroups (fractions) according to their molecular weight and physicochemical properties. The characteristics of each fraction are then related to its susceptibility to photocatalytic degradations

* Corresponding author phone: (+612) 9385-4361; fax: (+612) 9385-5966; e-mail: r.amal@unsw.edu.au.

[†] The University of New South Wales.

[‡] South Australian Water Corporation.

and the subsequent potential to form THMs and HAAs on reaction with chlorine. The comprehensive information derived from the current investigation was used to elucidate the characteristics of NOM that are more amenable to photocatalytic treatment. Subsequently, this could aid in the comparison of different treatment processes and improvement of existing treatment techniques. Moreover, with study of the profiles of organic compounds left at the end of photocatalytic treatment process and linking of them to the DBP formation potentials, the chemical characteristics of DBP precursors could be deduced. This may result in the possibility to gauge the propensity of the byproduct to form DBPs without having to carry out lengthy and costly analysis.

Materials and Methods

NOM Source. Water was collected from the Myponga Reservoir, a surface water source located 60 km south of Adelaide, Australia. The water samples were taken in the period of Australian winter (May 2007) and stored at 4 °C prior to experiments. Myponga water is generally high in color (85 HU) and DOC level (around 10 mg/L) and low in turbidity (2.3 NTU).

Reactor Setup. The AOP reactions were carried out in a laboratory-scale annular photoreactor with a volume of approximately 500 mL. A blacklight blue fluorescent lamp (NEC 20 W T10) with maximum emission at 365 nm is fitted through the center of the reactor. The photoreactor is connected to a 250 mL flask which serves as both a loading and sampling port by means of flexible tubings. Further details can be found in Liu et al. (21).

UVA/TiO₂ Degradation. TiO₂ suspension was prepared by mixing commercial-grade TiO₂ (Degussa P25) with Myponga water such that the final TiO₂ loading was 0.1 g/L. This TiO₂ loading was much lower than the optimum loading usually reported in the literature (1 g/L). The lower loading was chosen to attenuate the removal of NOM by TiO₂ adsorption and kinetically slow the photocatalytic reaction to ensure that changes can be properly monitored. The suspension pH was adjusted from 7.6 to 7 by using diluted perchloric acid solution. At a loading of 0.1 g/L TiO₂ and pH 7, the extent of NOM adsorption onto TiO₂ was found to be insignificant. An 800 mL volume of the prepared solution was transferred to the photoreactor and circulated within the reactor by a peristaltic pump. The degradation process was initiated by turning on the UV lamp and, for selected experiments, adding aliquots of 30% H₂O₂ such that the H₂O₂ concentration was 1 mM. This concentration was shown to be near the optimal point based on preliminary studies since the increase to 2 mM slowed down the kinetics of the photocatalytic degradation.

Over a period of time, 30 mL of the Myponga water samples were collected at 30 min interval and filtered through preirradiated 0.45 µm cellulose acetate membranes. The DOC of the samples was measured using a Sievers 820 Total Organic Carbon Analyzer (GE Analytical Instruments, USA). The absorbance spectra of the solution from 200 to 800 nm were determined using a UV–visible spectrophotometer (Cary 300).

High-Performance Size Exclusion Chromatography. The apparent molecular weight (AMW) distribution of samples was determined by HPSEC with UV detection. Sample injection and separation were conducted with a Waters 2690 Alliance system with a temperature-controlled oven (30 °C) and a Shodex KW802.5 glycol functionalized silica gel column. Elution was monitored with a Waters 996 photodiode array detector (260 nm). Samples were filtered through a 0.22 µm membrane filter prior to analysis and a sample volume of 100 µL was injected. The mobile phase was 0.02 M phosphate buffer at pH 6.8 adjusted to an ionic strength of 0.1 M with sodium chloride. The system was operated at isocratic

conditions with an eluent flow rate of 1.0 mL/min. Polystyrene sulfonate standards (Polysciences, USA) with MW 4.6, 8, 18, and 35 kDa were used to convert retention time response to apparent molecular weight.

Rapid Resin Fractionation. The fractionation setup as described in Chow et al. (22) was used to determine concentrations of the four NOM fractions prior to and at the end of the treatment process. Each sample was first passed through a 0.22 µm membrane to remove particulates and then the pH was adjusted to 2. The acidified sample was then passed onto a column packed with DAX-8 resin, which adsorbed the very hydrophobic acid (VHA) fraction. The effluent of the first column was passed to another column packed with XAD-4 resin to adsorb the slightly hydrophobic acid (SHA) fraction. A pH adjustment to 8 facilitated the selective adsorption of hydrophilic charged (CHA) fraction onto the third column packed with IRA-958 resin. The final effluent from the series of resins constituted the hydrophilic neutral (NEU) fraction. The concentration of VHA, SHA, and CHA fractions in the sample were determined by the difference in the influent and effluent DOC of each resin columns, which adsorb the specified fractions.

Trihalomethane Formation Potential (THMFP) Measurements. The THMFP measurement was carried out by reacting phosphate buffered water samples (pH 7.4) with excess of chlorine (approximately 20–30 mg/L). After incubation at 35 °C for 4 h, the sample was quenched with excess ascorbic acid. The THMs (chloroform, dichlorobromomethane, dibromochloromethane, and bromoform) were extracted using a solid-phase micro extraction (with 100 µm polydimethylsiloxane fiber) and their concentrations were determined by a Hewlett-Packard 6890 series GC system with a HP5973 Mass Selective Detector. Analyte separation was carried out with a HP-5MS capillary column (30.0 m × 250 µm i.d. × 0.25 µm film thickness).

Haloacetic Acid Analysis. The formation of haloacetic acids was carried out according to Standard Method 5710B (23), which involved buffering samples at neutral pH using phosphate solution, chlorinating the samples with excess free chlorine, and storing the sample at 25 °C for 7 days. The haloacetic acids formed were analyzed according to EPA Method 552.3 (24).

Aldehydes and Ketones Analysis. Carbonyl compounds in the raw and treated water were derivatized with *O*-2,3,4,5,6-(pentafluorobenzyl) hydroxylamine hydrochloride (PFBHA) and the oxime derivatives were subsequently extracted with hexane according to EPA Method 556. The analysis of the extracts was carried out using a HP6890 series GC system equipped with a HP5973 Mass Selective Detector and a HP-5MS capillary column, 30.0 m × 250 µm i.d. × 0.25 µm film thickness. Splitless injection of 1 µL was carried out using an autosampler (HP 7683 series) and a 10 µL glass syringe at 220 °C. The following temperature program was applied: 1 min at 50 °C, 4 °C/min to 220 °C, 20 °C/min to 250 °C, and holding for 10 min. The detector was set at 280 °C. Helium (pure carrier gas grade) was used as the carrier gas at a flow rate of 1.6 mL/min. GC/MS procedure was operated in the selected ion monitoring mode at *m/z* = 181. Identification of the PFBHA oxime derivatives was established by injecting pure standards in the same chromatographic conditions.

Results and Discussion

UVA/TiO₂ Degradation of Myponga Water. Figure 1 shows the DOC and UV₂₅₄ removal profile after TiO₂ photocatalytic oxidation at pH 7 with and without H₂O₂. It could be seen that a higher percentage of UV₂₅₄ removal was achieved compared to DOC removal, implying that the loss of aromaticity and conjugation is easier to achieve than mineralization of the NOM. This result is expected since NOM has a complex and heterogeneous composition, and therefore

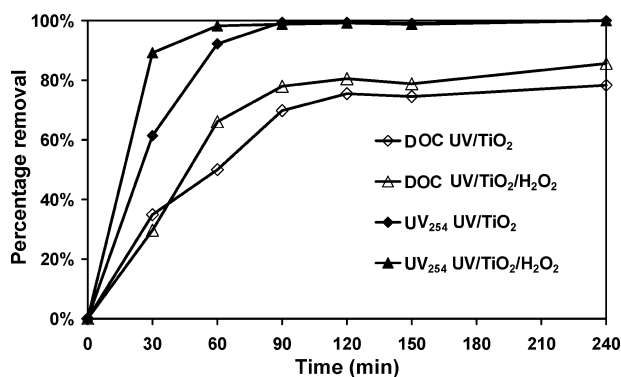


FIGURE 1. DOC and UV₂₅₄ removal for treatment with and without H₂O₂ (DOC of raw water = 10 mg/L).

the oxidation of NOM could generate a large amount of intermediates, which could have different reactivities toward oxidation compared to the original NOM. At the end of treatment, approximately 2 mg/L residual DOC remains in the water sample, indicating that complete mineralization could not be achieved. This may be due to the presence of refractory compounds in the original water sample or, alternatively, byproducts as a result of oxidation. The addition of hydrogen peroxide resulted in faster kinetics of photocatalytic degradation compared to the oxidation with TiO₂ alone, but residual DOC concentrations for the treatments with and without H₂O₂ are similar at the termination of the experiment. This was also observed in our previous work (21).

HPSEC Characterization of Myponga Water. Parts (a) and (b) of Figure 2 show that the chromatogram of untreated Myponga water has an AMW distribution of UV₂₆₀ active components consisting mostly of molecules in the 250–4000 Da range. The chromatogram was found to consist of three key peaks at approximately 300, 1350, and 6000 Da and two small shoulders at 750 and 1050 Da, respectively. Parts (c) and (d) of Figure 2 show the enlarged view of the low absorbing component of the chromatograms in (a) and (b) of Figure 2, respectively.

Parts (a) and (b) of Figure 2 also revealed that TiO₂ photocatalytic oxidation preferentially degraded the high molecular weight fractions of NOM, forming smaller byproducts, which were subsequently degraded after the larger MW organic matter was nearly depleted. This could be seen from the rapid decrease of the major peak at 1050 Da, after 30 min of irradiation. Photocatalytic treatment generally results in the shift of average molecular weight toward smaller molecular size. The addition of H₂O₂ to the photocatalytic system enhances the initial kinetics of the degradation reaction, as observed from the more rapid decrease in UV₂₆₀ absorbance after 30 min of illumination (Figure 2b). The presence of H₂O₂ in the combined UV/TiO₂/H₂O₂ treatment accelerates the degradation rate by generating extra hydroxyl radicals from its reaction with TiO₂ conduction band electrons (18) and inhibiting the recombination of electrons and holes.

After 90 min of irradiation, a small amount of organic matter with low AMW (200–1000 Da) was left, which remained even after 240 min of illumination. This clearly shows that the recalcitrant organic matter observed in both the DOC and UV₂₅₄ measurements are of this molecular size range. The less polydisperse peaks suggest that the heterogeneous mixture of organic molecules were degraded to a smaller group of compounds. As evident from (c) and (d) in Figure 2, the treatment with and without H₂O₂ has similar molecular weight distribution profiles, which suggests that although H₂O₂ addition may improve the initial degradation rate, it has less effect on oxidizing the lower AMW byproduct. The end products of both treatment processes are likely to

be similar. This is not surprising considering that the mechanism driving the UV/TiO₂ and UV/TiO₂/H₂O₂ treatments are also similar, namely, the preferential attack of hydroxyl radicals on larger molecules as a result of a higher number of reaction sites.

Rapid Resin Fractionation Analysis of Myponga Water.

Figure 3 illustrates the change in DOC concentrations of the four fractions after photocatalytic treatment at pH 7, with and without H₂O₂ addition, as a function of irradiation time. The rapid fractionation result indicates that the hydrophobic VHA fraction predominates the DOC composition of Myponga water sample: 4.8 mg/L of VHA (65% of DOC), with the SHA, CHA, and NEU fractions making up 1.5 mg/L (20% of DOC), 0.2 mg/L (3% of DOC), and 0.9 mg/L (12% of DOC), respectively. VHA and SHA fractions have been identified as humic acids and fulvic acids, respectively (22, 25). CHA fraction can be ascribed to proteins, amino acids, and anionic polysaccharides, while the NEU fraction can be ascribed to carbohydrates, aldehydes, ketones, and alcohols (22, 25).

A considerable decrease in the VHA fraction was observed after illumination, which suggests that this fraction is more prone to photocatalytic degradation than other fractions. This is also agreeable with the HPSEC results since the VHA fraction is composed of larger MW components, which are expected to be more readily degraded.

The DOC concentration of the SHA fraction, on the other hand, remains relatively steady at the early stage of the treatment when H₂O₂ is absent, and is only completely removed after 240 min of illumination. The DOC concentration of the CHA fraction shows a rapid increase from 0.2 mg/L (before treatment) to 2.1 mg/L after 30 min of UV/TiO₂ treatment, and reduces back to <0.5 mg/L at the end of 240 min of treatment. While VHA and SHA fractions continuously decrease following treatment, the concentration of CHA fraction increases substantially at the beginning, which implies that NOM degradation initially proceeds via breakup of high molecular weight, nonpolar fractions (VHA and SHA) to form lower molecular weight hydrophilic charged (CHA) fractions. The presence of H₂O₂ enhances the degradation rates, particularly in degrading the VHA and SHA fractions. However, H₂O₂ addition appeared to have little effect on the degradation of CHA and NEU fractions.

At the end of treatment, the organic matter which makes up the VHA and SHA fractions are degraded to undetectable levels. However, complete oxidation of the CHA and NEU fractions cannot be achieved even after 240 min of photocatalytic treatment. This indicates that the low molecular weight compounds observed after 90 min of irradiation in the HPSEC analysis could be composed of these hydrophilic charged or neutral molecules. The NEU fraction, which consists mostly of aldehydes, ketones, alcohols, and small carbohydrates, is particularly recalcitrant and has been reported to be slowly degraded by the TiO₂ photocatalytic process (26). The results from this study showed that photocatalytic oxidation changed the properties and composition of the DOC substantially. Over 90% of the DOC in Myponga water after photocatalytic treatment was classified as hydrophilic charged or neutral.

Aldehydes and Ketones Analysis. To assess the formation of aldehydes and ketones, which potentially make up the NEU fraction remaining at the end of the photocatalytic process, carbonyl analysis with PFBHA derivatization was performed. Figure 4 displays the evolution of aldehydes and ketones byproducts in raw and treated Myponga water. Some of the species have two peaks due to the presence of syn and anti stereoisomers, which are formed during the conversion of aldehydes into oximes. GC/MS analysis of the raw Myponga water revealed five detectable carbonyl compounds, which are formaldehyde, acetaldehyde, acetone, *n*-propanal, and *n*-butanal. After 150 min of irradiation time, the abundance

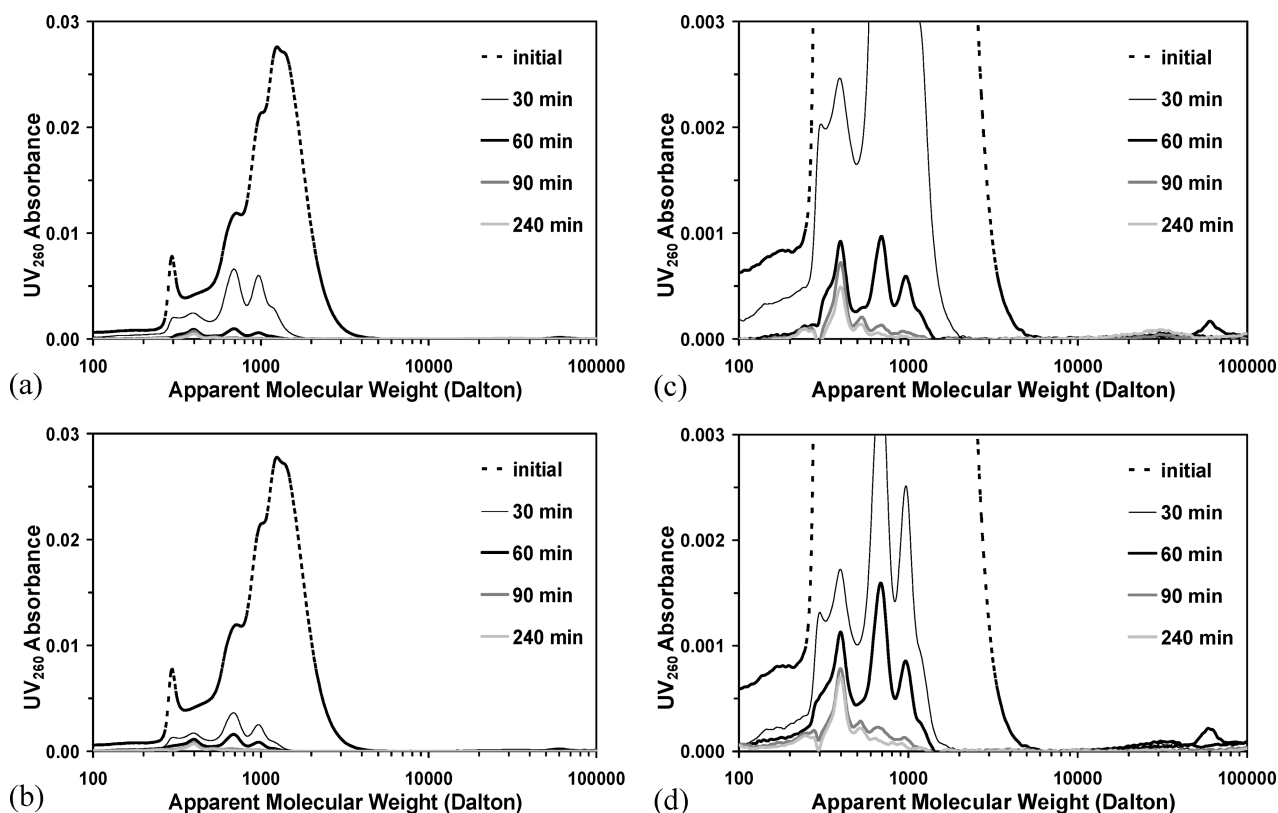


FIGURE 2. HPSEC chromatograms of water samples treated using (a) UVA/TiO₂ pH 7 and (b) UVA/TiO₂/H₂O₂ pH 7 after various periods of irradiation. (c) and (d) show the enlarged view of the low absorbing component of the chromatograms in (a) and (b), respectively.

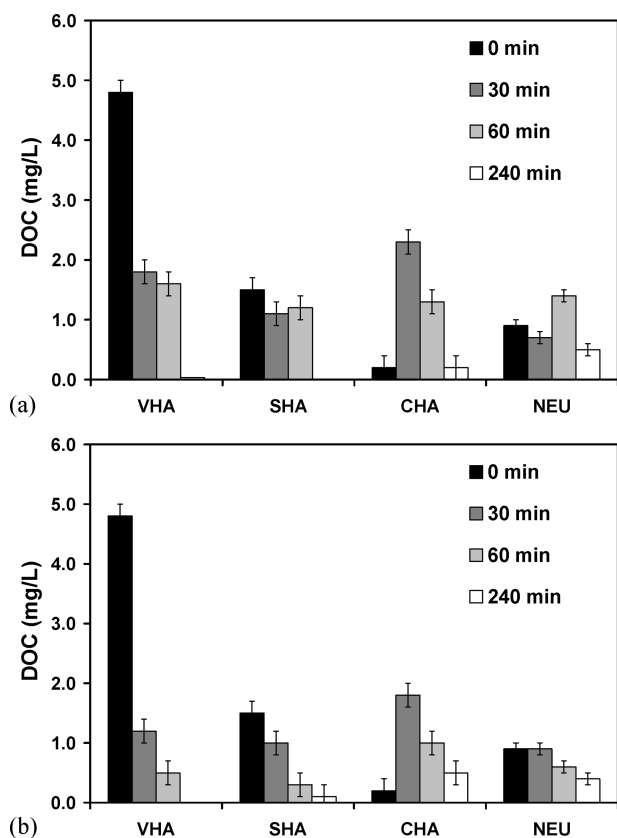


FIGURE 3. DOC concentrations of the VHA, SHA, CHA, and NEU fractions of Myponga water sample after (a) UVA/TiO₂ pH 7 and (b) UVA/TiO₂/H₂O₂ pH 7 treatments as a function of irradiation time.

of some carbonyl organic compounds, notably formaldehyde (Peak 1) and acetone (Peak 3), increased. This is not surprising since aldehydes and ketones are known to be typical byproducts or intermediates from the photocatalytic oxidation of large aromatic structures (27, 28). Some compounds are easily degraded, such as acetaldehyde, propanal, and butanal with retention times of 10.7, 13.4, and 16.2 min, respectively. The photocatalytic process oxidized the aldehydes and ketones byproducts to carboxylic acid, which in turn was mineralized to CO₂ and a carbon-centered radical (29). The reaction of this carbon-centered radical with photogenerated holes or hydroxyl radical could form alcohol byproducts, which were progressively degraded to form the corresponding aldehydes. This oxidation cycle yields increasingly shorter chain carbonyls, such as formaldehyde and acetone.

The abundance of longer chain aldehydes, such as propanal and butanal, are reduced significantly, as observed from the absence of peaks which elute at 13.4 and 16.2 min, respectively. This is consistent with the HPSEC results where a rapid decrease in the apparent molecular weight distribution of the organic material was observed upon photocatalytic treatment. In addition, these observations are in agreement with the rapid fractionation results which indicate that carbonyl compounds such as short chain aldehydes and ketones, which are key components of the NEU fraction, remain at the end of 150 min of photocatalytic treatment.

Disinfection Byproducts Formation. The total THMFP as a function of irradiation time was measured to assess the reactivity of product with chlorine at the different stages of the photocatalytic treatment. The change in the trihalomethanes level of the Myponga water after UV/TiO₂ pH 7 and UV/TiO₂/H₂O₂ pH 7 treatments with time were reported in Figure 5.

It could be seen from Figure 5 that the total THMFPs after treatment were substantially less than that of the raw

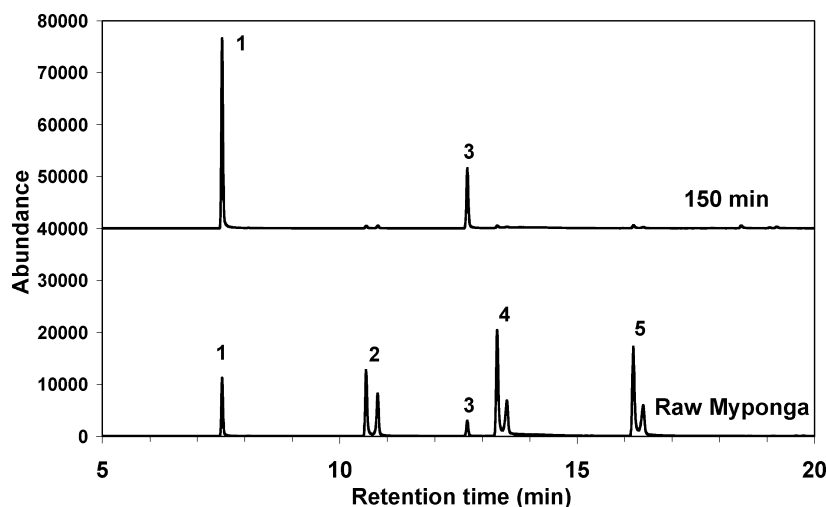


FIGURE 4. The GC-MS SIM (m/z 181) chromatograms of aldehydes and ketones PFBHA oximes in raw Myponga water and treated water. Peaks: 1 = formaldehyde, 2 = acetaldehyde, 3 = acetone, 4 = propanal, 5 = butanal.

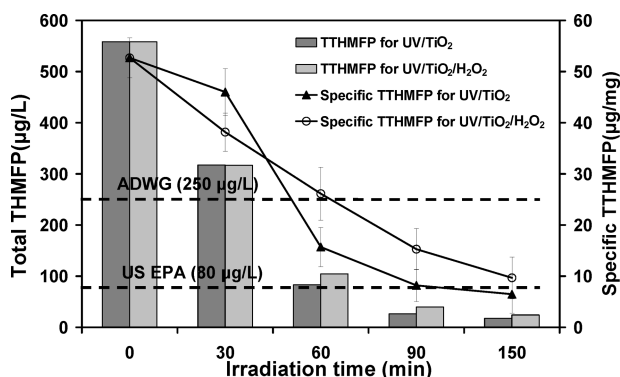


FIGURE 5. Total THMFP (TTHMFP) and specific TTHMFP concentration in Myponga water sample before and after treatment.

Myponga water, which was $558 \mu\text{g/L}$. In both UV/TiO_2 and $\text{UV}/\text{TiO}_2/\text{H}_2\text{O}_2$ processes, the total THMFP dropped by approximately $241 \mu\text{g/L}$ from the initial value in the first 30 min, $454\text{--}475 \mu\text{g/L}$ after 60 min, and $534\text{--}541 \mu\text{g/L}$ after 90 min of the photocatalytic degradation process. Chloroform formed the majority of trihalomethane species, followed by dichlorobromomethane and dibromochloromethane. The concentration of bromoform in the raw and treated Myponga water samples was below the detection limit.

At the end of treatment, only about $20 \mu\text{g/L}$ of total THMs was formed, demonstrating the efficient removal of THM precursors. The low TTHMFP concentration after the photocatalytic treatment is consistent with the significantly reduced DOC concentration and UV absorbance after oxidation. The percentage removal of trihalomethane formation potential exceeds the percentage removal of TOC, as indicated by a decrease in the specific TTHMFP from 56 to $10 \mu\text{g/mg}$, which suggests that the organic moieties which form trihalomethanes are susceptible to photocatalytic treatment. Although complete mineralization could not be achieved, the photocatalytic oxidation induces changes to the chemical structure of THM precursors to compounds that are less reactive to chlorine. No significant difference in the total THMFP concentration was observed for the UV/TiO_2 process with and without H_2O_2 . This implies that the addition of H_2O_2 to the photocatalytic treatment does not change the degradation products despite the improvement in reaction kinetics.

In contrast to THMFP, the HAAFP after photocatalytic treatment of NOM has not been extensively studied. Bekbolet

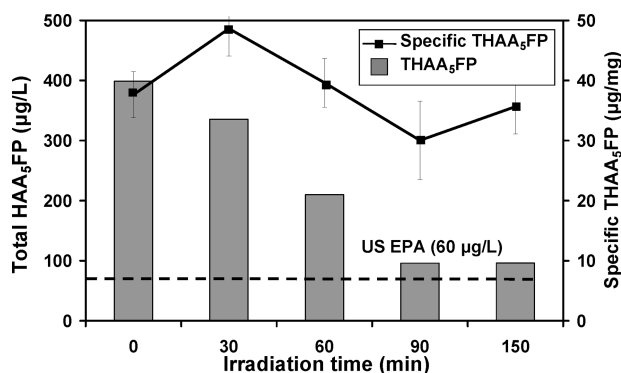


FIGURE 6. Total HAA₅FP and specific THAA₅FP concentrations in Myponga water sample before and after photocatalytic treatment.

et al. (30) compared the formation potentials of four HAA species: chloroacetic acid, dichloroacetic acid, trichloroacetic acid, and dibromoacetic acid in raw water taken from different regions of Istanbul (Turkey) and their corresponding treated water by photocatalytic treatment. They found that, after photocatalysis, the formation of trichloroacetic acid was enhanced.

Although there are nine HAA species, only five (HAA₅) are currently regulated by the U.S. Environmental Protection Agency (U.S. EPA), which are chloroacetic acid, dichloroacetic acid, trichloroacetic acid, bromoacetic acid, and dibromoacetic acid. Figure 6 displays the changes in the concentration of haloacetic acids formed from untreated and photocatalytically treated water after spiking with chlorine. Dichloroacetic acid and trichloroacetic acid represented 84% of the total HAA₅FP in the raw Myponga water. All the remaining HAA₅ exist in minor proportions. A significant decrease in the concentration of HAA₅FP was observed, from $400 \mu\text{g/L}$ for water before treatment to $100 \mu\text{g/L}$ for water irradiated for 150 min. This is over the $60 \mu\text{g/L}$ limit imposed by the U.S. EPA, under the Stage 2 Disinfection/Disinfection By-Product (D/DBP) Rule, but still under the limits set by the Australian Drinking Water Guidelines (31), which specify only three species of HAAs: namely, $150 \mu\text{g/L}$ for chloroacetic acid, $100 \mu\text{g/L}$ for dichloroacetic acid, and $100 \mu\text{g/L}$ for trichloroacetic acid. Moreover, it should be noted that the high chlorine dosage used in this study is likely to overestimate the amount of HAAs likely to be formed in the water.

At the initial stage of the photocatalytic oxidation, the specific THAA₅FP increased from $38 \mu\text{g/mg}$, which

indicates the formation of photocatalytic intermediates that had greater tendency to form HAAs. With prolonged irradiation, specific THAA₅FP reverted back to its initial value and remained relatively constant. The distinction in the trend of specific TTHMFP and specific THAA₅FP with increasing irradiation time highlights the difference between the structure and chemical functionality of THMs and HAAs precursors, which ultimately govern their reactivity with chlorine. The increase in the specific THAA₅FP can be attributed to the increase in hydrophilic substituents during the photocatalytic oxidation process (see Figure 3), which has been reported to be the major precursor of HAAs (32).

This work provides an improved understanding of the organic characteristics and byproducts of NOM after TiO₂ photocatalytic oxidation through several complementary analytical techniques. The photocatalytic oxidation of Myponga water transformed large aromatic organic structures in the water to smaller and more hydrophilic organics. Although the specific THAAFP of the treated water remained relatively constant, the specific THMFP was reduced drastically. This indicates the superiority of TiO₂ photocatalysis for reducing THMs precursors compared to HAAs precursors in Myponga water.

Acknowledgments

We acknowledge Edith Kozlik for assisting with analytical work, Dr. Gautam Chattopadhyay for help in GC/MS analysis, and ARC Centre of Excellence for Functional Nanomaterials for financial support.

Literature Cited

- (1) Stevenson, F. J. *Humus Chemistry: Genesis, Composition, Reactions*; John Wiley and Sons: New York, 1994.
- (2) Karanfil, T.; Kitis, M.; Kilduff, J. E.; Wigton, A. Role of granular activated carbon surface chemistry on the adsorption of organic compounds. 2. Natural organic matter. *Environ. Sci. Technol.* **1999**, 33 (18), 3225–3233.
- (3) Yoon, S. H.; Lee, C. H.; Kim, K. J.; Fane, A. G. Effects of calcium ion on the fouling of nanofilter by humic acid in drinking water production. *Water Res.* **1998**, 32 (7), 2180–2186.
- (4) Richardson, S. D. Drinking water disinfection by-products. In *Encyclopedia of Environmental Analysis and Remediation*; Wiley: New York, 1998; pp 1398–1421.
- (5) Thurman, E. M. *Organic Geochemistry of Natural Waters*; Nijhoff: Boston, 1985.
- (6) Aiken, G. R.; McKnight, D. M.; Wershaw, R. L.; MacCarthy, P. *Humic Substances in Soil, Sediment, and Water: Geochemistry, Isolation, and Characterization*; John Wiley: New York, 1985.
- (7) Uyak, V.; Toroz, I. Disinfection by-product precursors reduction by various coagulation techniques in Istanbul water supplies. *J. Hazard. Mater.* **2007**, 141 (1), 320–328.
- (8) Bolto, B.; Dixon, D.; Eldridge, R. Ion exchange for the removal of natural organic matter. *React. Funct. Polym.* **2004**, 60, 171–182.
- (9) Schafer, A. I.; Fane, A. G.; Waite, T. D. Cost factors and chemical pretreatment effects in the membrane filtration of waters containing natural organic matter. *Water Res.* **2001**, 35 (6), 1509–1517.
- (10) Matilainen, A.; Vieno, N.; Tuhkanen, T. Efficiency of the activated carbon filtration in the natural organic matter removal. *Environ. Int.* **2006**, 32 (3), 324.
- (11) Siddiqui, M. S.; Amy, G. L.; Murphy, B. D. Ozone enhanced removal of natural organic matter from drinking water sources. *Water Res.* **1997**, 31 (12), 3098–3106.
- (12) Toor, R.; Mohseni, M. UV-H₂O₂ based AOP and its integration with biological activated carbon treatment for DBP reduction in drinking water. *Chemosphere* **2007**, 66 (11), 2087–2095.
- (13) Fearing, D. A.; Banks, J.; Guyetand, S.; Monfort Eroles, C.; Jefferson, B.; Wilson, D.; Hillis, P.; Campbell, A. T.; Parsons, S. A. Combination of ferric and MIEEX for the treatment of a humic rich water. *Water Res.* **2004**, 38 (10), 2551–2558.
- (14) Kabsch-Korbutowicz, M. Application of ultrafiltration integrated with coagulation for improved NOM removal. *Desalination* **2005**, 174, 13–22.
- (15) Eggins, B. R.; Palmer, F. L.; Byrne, J. A. Photocatalytic treatment of humic substances in drinking water. *Water Res.* **1997**, 31 (5), 1223.
- (16) Bekbolet, M.; Ozkosemen, G. A preliminary investigation on the photocatalytic degradation of a model humic acid. *Water Sci. Technol.* **1996**, 33 (6), 189–194.
- (17) Palmer, F. L.; Eggins, B. R.; Coleman, H. M. The effect of operational parameters on the photocatalytic degradation of humic acid. *J. Photochem. Photobiol., A: Chem.* **2002**, 148, 137–143.
- (18) Bekbolet, M.; Balcioglu, I. Photocatalytic degradation kinetics of humic acid in aqueous TiO₂ dispersions: The influence of hydrogen peroxide and bicarbonate ion. *Water Sci. Technol.* **1996**, 34 (9), 73–80.
- (19) Wiszniowski, J.; Robert, D.; Surmacz-Gorska, J.; Miksch, K.; Weber, J.-V. Photocatalytic mineralization of humic acids with TiO₂: Effect of pH, sulfate and chloride anions. *Int. J. Photoenergy* **2003**, 5 (2), 69–74.
- (20) McDonald, S.; Bishop, A. G.; Prenzler, P. D.; Robards, K. Analytical chemistry of freshwater humic substances. *Anal. Chim. Acta* **2004**, 527, 105–124.
- (21) Liu, S.; Lim, M.; Fabris, R.; Chow, C.; Chiang, K.; Drikas, M.; Amal, R. Removal of humic acid using TiO₂ photocatalytic process - Fractionation and molecular weight characterisation studies. *Chemosphere* **2008**, 72 (2), 263–271.
- (22) Chow, C. W. K.; Fabris, R.; Drikas, M. A rapid fractionation technique to characterise natural organic matter for the optimisation of water treatment processes. *J. Water SRT-AQUA* **2004**, 53 (2), 85–92.
- (23) APHA. *Standard Methods for the Examination of Water and Wastewater*, 20th ed.; APHA-AWWA-WEF: Washington, D.C., 1998.
- (24) Domino, M. M.; Pepich, B. V.; Munch, D. J.; Fair, P. S.; Xie, Y. EPA METHOD 552.3, Revision 1.0, Determination of Haloacetic Acids and Dalapon in Drinking Water by Liquid-Liquid Micro Extraction, Derivatization, and Gas Chromatography with Electron Capture Detection; EPA 815-B-030-002; U.S. Environmental Protection Agency: Cincinnati, OH, 2003.
- (25) Croue, J. P.; Martin, B.; Deguin, A.; Legube, B. Isolation and characterisation of dissolved hydrophobic and hydrophilic organic substances of a reservoir water. In *Natural Organic Matter in Drinking Water*; American Water Works Association: Denver, 1994; p 73.
- (26) Tran, H.; Scott, J.; Chiang, K.; Amal, R. Clarifying the role of silver deposits on titania for the photocatalytic mineralisation of organic compounds. *J. Photochem. Photobiol., A: Chem.* **2006**, 183, 41.
- (27) Ho, P. C. Photooxidation of 2,4-dinitrotoluene in aqueous solution in the presence of hydrogen peroxide. *Environ. Sci. Technol.* **1986**, 20 (3), 260–267.
- (28) Wang, Y.; Hong, C.-S. TiO₂-mediated photomineralization of 2-chlorobiphenyl: the role of O₂. *Water Res.* **2000**, 34 (10), 2791–2797.
- (29) Denny, F.; Scott, J.; Chiang, K.; Teoh, W. Y.; Amal, R. Insight towards the role of platinum in the photocatalytic mineralisation of organic compounds. *J. Mol. Catal. A: Chem.* **2007**, 263 (1–2), 93–102.
- (30) Bekbolet, M.; Uyguner, C. S.; Selcuk, H.; Rizzo, L.; Nikolaou, A. D.; Meric, S.; Belgiorno, V. Application of oxidative removal of NOM to drinking water and formation of disinfection by-products. *Desalination* **2005**, 176 (1–3), 155–166.
- (31) ADWG, Australian Drinking Water Guidelines 6; NHMRC and ARMCANZ: Canberra, ACT, 2004.
- (32) Hwang, C. J.; Scilimenti, M. J.; Bruchet, A.; Croué, J. P.; Amy, G. L. DBP yields of polar NOM fractions from low humic waters. In *Proceedings of Water Quality Technology Conference*; AWWA: Denver, CO, 2001.

ES800887S